Journal of Colloid and Interface Science **249,** 476–480 (2002)
doi:10.1006/jcis.2002.8292, available online at http://www.idealibrary.com on IDEAL®

Bubble Shapes and Orientations in Low Re Simple Shear Flow

A. C. Rust*,[1] and Michael Manga†

*Department of Geological Sciences, 1272 University of Oregon, Eugene, Oregon 97403; and †Department of Earth and Planetary Science, University of California, Berkeley

Received November 12, 2001; accepted February 7, 2002; published online April 10, 2002

We present measurements of shape and orientation of air bubbles in a viscous Newtonian fluid deformed by simple shear. The apparatus is a variation of the "parallel band" device developed by G. I. Taylor. Previous experimental studies on low viscosity ratio, low Reynolds number (Re $\ll 1$) bubble deformation have focussed on either small or large deformations (mostly small deformation) and have only qualitatively examined the orientation of bubbles except for small deformations. Our data set spans both the theoretical small deformation and high deformation limits. With these data we confirm theoretical relationships and assess the range of capillary numbers (Ca) over which theoretical relationships for shape and orientation of bubbles are appropriate. We also examine the geometry of deformed bubbles as they relax to a spherical shape once shear stresses are removed. Our data indicate that for extremely small Reynolds numbers and viscosity ratios, the small deformation theoretical relationship first developed by Taylor, is a good approximation for Ca < 0.5. The large deformation results for both shape and bubble orientation derived by Hinch and Acrivos agree with our data for Ca > 1 and Ca > 0.5, respectively.

Key Words: **bubble; deformation; simple shear; capillary number; shape relaxation.**

INTRODUCTION

Analysis of the deformation of bubbles suspended in sheared, high viscosity fluids is relevant to the processing of polymer melts, foods, and biological materials (1, 2). Another application, and the impetus for the present study, is determining flow dynamics of volcanic processes (e.g., lava flows) from the geometry of bubbles preserved in glassy rocks (3). In this paper we present results of experiments on the deformation of air bubbles in corn syrup under simple shear. The syrup is Newtonian, lacks surfactants (4), and is dominated by viscous rather than inertial forces at the scale of the bubbles and shear rates of the experiments (Reynolds number $\ll 1$).

An initially spherical bubble placed in a low Reynolds number, steady simple shear flow deforms with a time-dependent shape and orientation until it reaches a steady geometry or breaks into smaller bubbles. The steady bubble shape and orientation depend on (i) the ratio of the viscosities of the bubble relative to the ambient fluid (this viscosity ratio is denoted λ), (ii) the concentration and behavior of surfactants, and (iii) the capillary number, Ca, the ratio of shear stresses that deform bubbles to the surface tension stresses that tend to keep bubbles spherical (e.g., see review by Stone (2)). There is some critical Ca, $\mathrm{Ca_{cr}}$, which increases with decreasing λ, beyond which a bubble cannot maintain a steady shape but deforms continuously and then breaks into multiple bubbles (e.g., 5).

Most numerical simulations and previous experimental studies for Re $\ll 1$ deformation in simple shear have emphasized small deformations or drop breakup because viscosity ratios were modest (6–10). In the experiments reported here, $\lambda = \mathrm{O}(10^{-7})$. Based on experimental and theoretical models for $\mathrm{Ca_{cr}}$ (e.g., 5, 11, 12), bubbles with such low viscosity ratios are expected to reach a stable shape rather than break in steady shear flow up to $\mathrm{Ca} = \mathrm{O}(10^3)$. As we are dealing with surfactant-free systems with $\lambda \to 0$, the steady geometry of the bubbles is solely a function of Ca, which is calculated by

$$\mathrm{Ca} = \frac{aG\mu_s}{\Gamma}, \qquad [1]$$

where a is the nondeformed bubble radius, G is the shear rate, μ_s is the suspending fluid viscosity, and Γ is the surface tension.

The flow-induced orientation of a bubble with respect to the shear flow is described by the angle θ between the principal axis of the bubble (longest dimension) and the shear direction, measured in a plane containing both the shear direction and the velocity gradient (Fig. 1). In contrast to pure shear, in simple shear θ varies with Ca. For slightly deformed bubbles (Ca $\ll 1$), $\theta = 45^\circ$ and θ decreases as Ca increases (e.g., 13). Rallison (14) found the first order correction to the orientation using a perturbation analysis. For Ca $\ll 1$ and $\lambda \ll 1$ Rallison (14) predicts

$$\theta = \frac{\pi}{4} - 0.6\mathrm{Ca}, \qquad [2]$$

a result confirmed experimentally by Guido and Greco (15). Using slender-body theory, Hinch and Acrivos (12) predict that for high capillary numbers and $\lambda \ll 1$,

$$\theta = \tan^{-1}\left(0.359\mathrm{Ca}^{3/4}\right). \qquad [3]$$

The magnitude of flow-induced bubble deformation is generally quantified with one of two dimensionless parameters, $D = (l - b)/(l + b)$ or l/a, where l and b are the semi-major and semi-minor axes of the sheared bubble, respectively. These

[1] To whom correspondence should be addressed.

0021-9797/02 $35.00

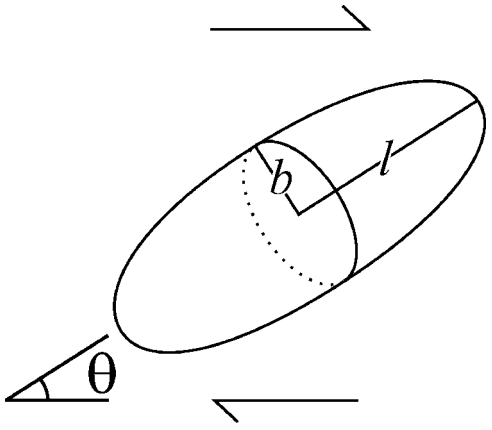

FIG. 1. Schematic of a deformed bubble in a simple shear flow field.

deformation parameters are not independent but D is convenient for small deformations ($\mathrm{Ca} \ll 1$) and l/a is useful for $\mathrm{Ca} \gg 1$. For $\mathrm{Ca} \ll 1$ and $\lambda \ll 1$, the bubble is nearly spherical with

$$\mathrm{Ca} \cong D \qquad [4]$$

(e.g., 16–18). Experimental data (5, 11, 15, 17, 19–21) and numerical calculations (22–26) confirm Eq. [4].

At high deformations ($l \gg a$), bubbles are elongate with pointed ends. Using slender body theory and assuming bubbles are circular in cross section, Hinch and Acrivos (12) predict

$$\frac{l}{a} \cong 3.45\mathrm{Ca}^{1/2} \qquad [5]$$

for $\mathrm{Ca} \gg 1$, $\lambda \ll 1$, and $\mathrm{Re} \ll 1$. Canedo *et al*. (1) measured experimentally the deformation of air bubbles suspended in polybutene oil in a Couette device (which approximates simple shear). Canedo *et al*. (1) found that bubble cross-sections are elliptical and suggested that deformations as a function of Ca are slightly less than predicted by Eq. [5]. Their data ($3 < \mathrm{Ca} < 50$) are well described by

$$\frac{l}{a} = 3.1\mathrm{Ca}^{0.43}. \qquad [6]$$

Our experiments on bubble deformation in simple shear comprise orientation and shape data for $0.02 < \mathrm{Ca} < 7.1$. Previous experimental and numerical studies on $\lambda \ll 1$, $\mathrm{Re} \ll 1$ bubble deformation have focussed on either small or large deformations (mostly small deformation) and have only qualitatively examined the orientation of bubbles as a function of Ca except at $\mathrm{Ca} < 1$ and λ of order 1 (15). Our data set reaches both the spheroidal and slender body model regimes (Eqs. [4] and [5], respectively) as well as the transition between these small and large deformation limits. We also examine the geometry of deformed bubbles as they reround once shear stresses are removed.

APPARATUS AND METHOD

The apparatus is based on the "parallel band" device of Taylor (17) but generates a simple shear flow with one rather than two bands. The band is a loop of 35mm photographic film extended between a guiding spool and a projector sprocket with teeth that engage with perforations in the film (Fig. 2). A variable speed motor attached to the sprocket drives the film belt. The device is enclosed in a transparent acrylic tank filled with corn syrup. Far from the rotating spools, a simple shear flow is produced in the syrup encompassed by the loop of film (Fig. 2b). Half way between the two parallel sides of the film loop, the velocity is zero and the position of a bubble placed there remains constant as it deforms by simple shear.

Individual air bubbles are injected with a needle and syringe into the syrup in the center of the stationary film loop. The film belt is set in motion at a constant rotation rate until a steady bubble shape is achieved. The rotation rate is increased and left constant until the bubble reaches a new steady shape. This process is repeated at progressively higher shear rates until the bubble approaches the top of the film loop due to buoyancy. The motor is then turned off and the bubble relaxes to a sphere. The entire experiment is recorded with a digital video camera. The bubble size, shape, and orientation relative to the film belt are measured from images captured from the video footage.

RESULTS

To examine relationships between bubble geometry and Ca, we combine data from experiments on 15 bubbles ($0.88 \leq a \leq 2.55$ mm), each of which was subjected to a different set of shear rates ($0.00921 \leq G \leq 1.77\ \mathrm{s}^{-1}$). The viscosity of the corn syrup at the temperature of the experiments was determined with a Cole Parmer 98936 series rotational viscometer. Eleven of the bubbles were deformed in syrup with a viscosity of 137 Pa s. The other four bubbles were suspended in slightly less viscous syrup ($\mu = 118$ Pa s).

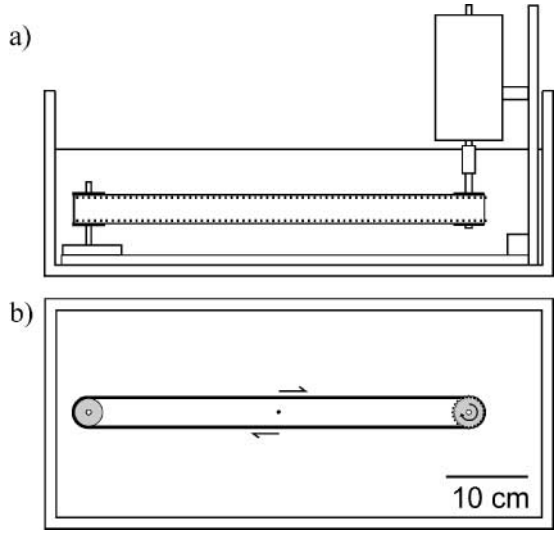

FIG. 2. The apparatus viewed from (a) the side and (b) above. A motor drives a belt of 35 mm photographic film in a tank of corn syrup. A bubble injected into the center of the film loop is deformed by simple shear.

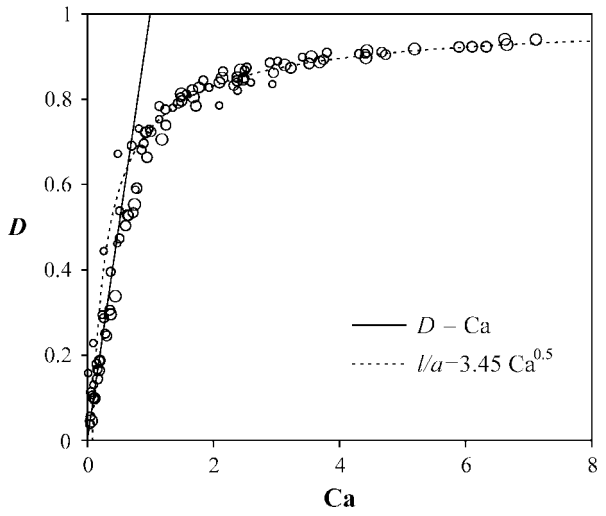

FIG. 3. Deformation parameter, $D = (l - b)/(l + b)$, vs capillary number for bubbles in steady simple shear flow with $\lambda \ll 1$ and $\mathrm{Re} \ll 1$. The size of each circle is proportional to that of the undeformed bubble it represents ($0.88 \leq a \leq 2.55$ mm). The solid line is the small deformation theory, $D = \mathrm{Ca}$ (e.g., 17). The dashed curve is the high deformation prediction by (12), converted to $D(\mathrm{Ca})$ assuming bubbles are ellipsoids with circular cross-sections.

As a and G are known, the only additional parameter required for the calculation of Ca is surface tension. Borhan and Pallinti (27) measured Γ between air and corn syrup with a ring tensiomenter to be 0.0808 N/m. We determine Γ for our fluids using the approximation $D = \mathrm{Ca}$ for small Ca (17). A least squared residual fit for $D = (\mu a G)/\Gamma$ using data with $D < 0.4$ data results in $\Gamma = 0.082 \pm 0.002$ N/m.

The steady deformations of the bubbles as a function of Ca are plotted in Figs. 3 and 4. As predicted by Taylor (17), the deformation parameter, D, scales with Ca for small Ca (Fig. 3). This relationship holds up to Ca approximately 0.5, above which $\mathrm{d}D/\mathrm{dCa}$ decreases and D approaches 1. Experiments by Torza *et al.* (19) and calculations by Kennedy *et al.* (18) for drops in simple shear with $\lambda = 0.08$ or greater show increasing $\mathrm{d}D/\mathrm{dCa}$ with increasing Ca. This disparity is explained by the significantly lower viscosity ratio of our experiments ($\lambda = \mathrm{O}(10^{-7})$) such that Capillary numbers are not approaching the critical Ca, $\mathrm{Ca_{cr}}$, for bubble breakup. In our experiments, bubble deformations reach $D = 0.94$ ($l/b = 32$) but no bubble breakup occurred during shearing (motor on) or bubble shape relaxation (motor off).

Figure 4 shows that the $\mathrm{Ca} > 1$ data are consistent with the theoretical relationship for $l/a \gg 1$, $\lambda \ll 1$, $\mathrm{Re} \ll 1$ predicted by Hinch and Acrivos (12). The best-fit relationship obtained by Canedo *et al.* (1), also shown in Fig. 4, underestimates our data, perhaps due to the curvature of the streamlines and bubbles in their Couette device.

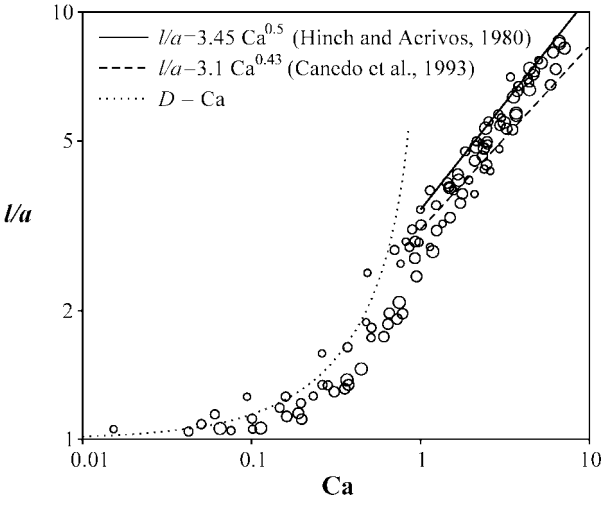

FIG. 4. Dimensionless extension ratio (l/a) vs capillary number, for bubbles in steady simple shear flow with $\lambda \ll 1$ and $\mathrm{Re} \ll 1$. The size of each circle is proportional to that of the undeformed bubble it represents ($0.88 \leq a \leq 2.55$ mm). The solid line is the prediction by Hinch and Acrivos (12) based on slender body theory. The dashed line is the best fit for Canedo *et al.* (1) data ($3 < \mathrm{Ca} < 50$). The dotted curve is the small deformation theory $D = \mathrm{Ca}$, converted to l/a assuming bubbles are ellipsoids with circular cross-sections.

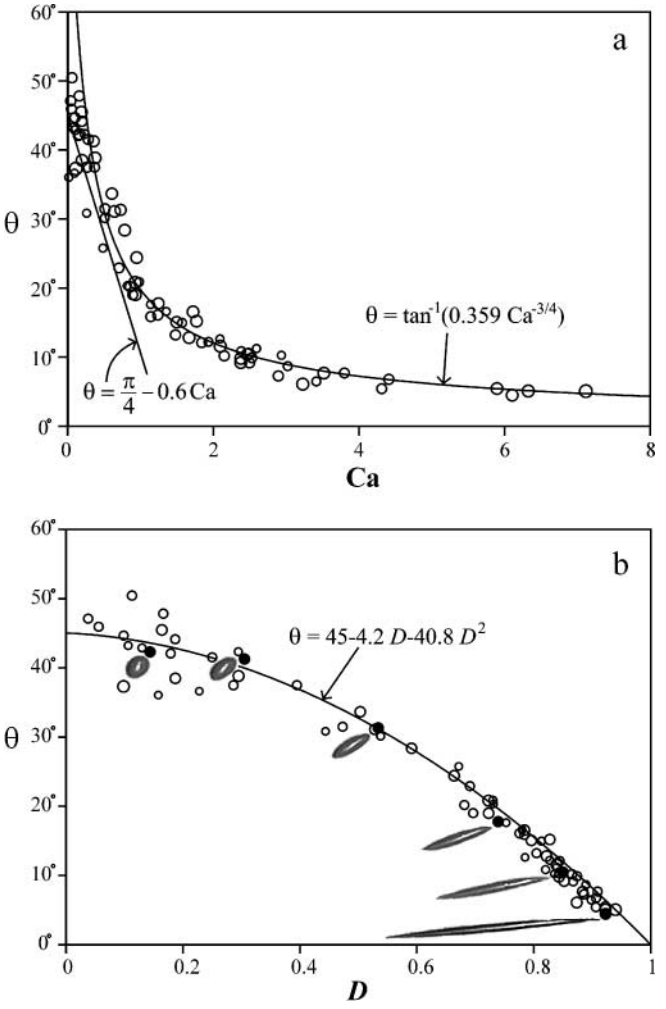

FIG. 5. The steady orientations of bubbles in simple shear flow as a function of Ca and D. (a) The line and curve are theoretical relationships for $\theta(\mathrm{Ca})$ at low and high deformations respectively with θ in radians (see text for details). (b) The curve is an empirical equation for $\theta(D)$ for all possible D with θ in degrees.

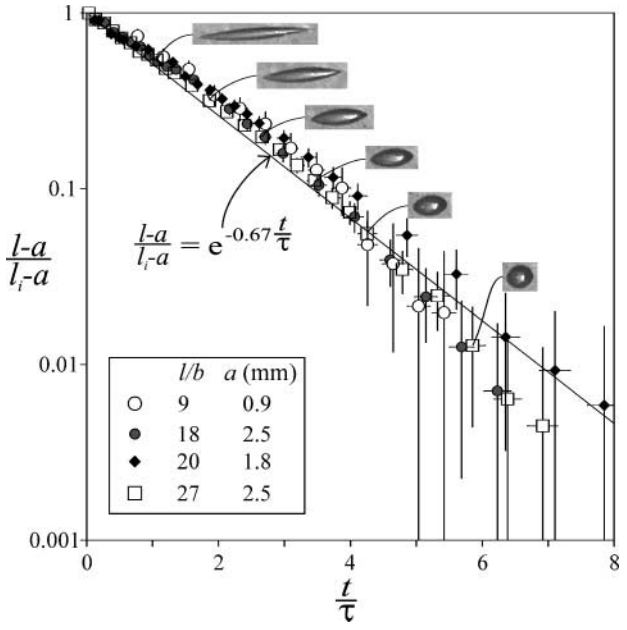

FIG. 6. The relaxation of bubble shape after shear flow is ceased (motor turned off). The four bubbles of radii, $a = 0.9$, 2.5, 1.8, and 2.5 mm, began with aspect ratios (l/b) of 9, 18, 20, and 27, respectively. All bubbles were suspended in syrup with a viscosity of 118 Pa s. See text for details on nondimensionalization of bubble elongation and time. The curve is an exponential fit to the entire data set (Eq. [8]). The bubble photographs are for the bubble with an initial aspect ratio of 27 (square symbols).

The orientations of the bubbles relative to the shear direction (θ) are shown in Fig. 5 as a function of Ca and D. As expected, in the limit of zero shear ($D \to 0$ and Ca$\to$ 0), $\theta \approx 45^\circ$, and θ decreases toward zero as Ca increases (e.g., 13). The data fit the theoretical high Ca relationship (Eq. [3]) remarkably well down to Ca as low as 0.5. We examine θ as a function of D in addition to Ca for the purposes of comparison with data from bubbles in natural volcanic glass samples (the original motivation of our analyses) because D can be calculated directly from bubble dimensions without estimates of a, μ_s, Γ, and shear type. The data are well described by $\theta = 45 - 4.2D - 40.8D^2$ for θ in degrees.

When the shear stress deforming a bubble is removed, the bubble shape relaxes due to surface tension until it is spherical, the geometry with the minimum surface area. As its shape relaxes, the bubble remains at the orientation it had when the shear stress was removed. In Fig. 6 we examine the relaxation of four bubbles with different initial aspect ratios and radii (l/b, a(mm) = 27, 2.5; 20, 1.8; 18, 2.5; and 9, 0.9). To collapse the data sets to a single curve we plot $(l - a)/(l_i - a)$ versus t/τ, where l_i is the initial (steady) length, l, prior to relaxation, t is time, and τ is the surface tension timescale (e.g., 15) also sometimes referred to as the characteristic relaxation time (e.g., 28) which is calculated by

$$\tau = \frac{a\mu_s}{\Gamma}. \qquad [7]$$

An exponential fit to the data constrained to include $(l - a)/(l_i - a) = 1$ is

$$\frac{l-a}{l_i-a} = e^{-0.67\frac{t}{\tau}}. \qquad [8]$$

Despite their small radius of curvature, the ends of the bubbles remain pointed through substantial reduction in aspect ratio (Fig. 6). For the same magnitude of deformation (l/a, l/b or D), a steady bubble in a shear flow has shorter l and b and more pointed ends than a bubble that has relaxed from a more deformed state. The shorter l and b are due to the noncircular cross-section (perpendicular to maximum elongation) of steady bubbles deformed in simple shear (e.g., 1).

SUMMARY

Our experimental study of $\lambda \ll 1$ bubble deformation in Re $\ll 1$ simple shear flow spans both the small deformation and high deformation limits. With these data we can assess the range of Ca over which theoretical relationships for shape and orientation of bubbles are appropriate.

In particular our data indicate that for simple shear with $\lambda \to 0$ and Re $\ll 1$, the small deformation theoretical relationship $D \cong$ Ca is a good assumption for Ca < 0.5. The large deformation results for shape and orientation developed by Hinch and Acrivos (12) are good approximations for Ca > 1.0 and 0.5, respectively. A second order polynomial fit to the $\theta(D)$ data yields the empirical equation $\theta = 45 - 4.2D - 40.8D^2$ for θ in degrees and $0 < D < 1$.

ACKNOWLEDGMENTS

This work was supported by NSF Grant EAR0003303 (M. Manga) and a NSERC PGSB award (A. Rust). D. Senkovich and K. Johnson provided technical assistance.

REFERENCES

1. Canedo, E. L., Favelukis, M., Tadmor, Z., and Talmon, Y., *AIChE* **39,** 553 (1993).
2. Stone, H. A., *Ann. Rev. Fluid Mech.* **26,** 65 (1994).
3. Manga, M., Castro, J., Cashman, K. V., and Loewenberg, M., *J. Volcanol. Geotherm. Res.* **87,** 15 (1998).
4. Rust, A. C., and Manga, M., *J. NonNewt. Fluid Mech.*, in press.
5. Bentley, B. J., and Leal, L. G., *J. Fluid Mech.* **167,** 241 (1986).
6. Bigio, D. I., Marks, C. R., and Calabrese, R. V., *Int. Polymer Proc.* **13** 192 (1998).
7. Kwak, S., and Pozrikidis, C., *J. Comp. Phys.* **145,** 61 (1998).
8. Marks, C. R., Ph.D. thesis, University of Maryland, College Park, 1998.
9. Zinchenko, A. Z., Rother, M. A., and Davis, R. H., *J. Fluid Mech.* **391,** 249 (1999).
10. Li, J., Renardy, Y. Y., and Renardy, M., *Phys. Fluids* **12,** 269 (2000).
11. Grace, H. P., *in* "Eng. Found. Res. Conf. Mixing, 3rd, Andover, NH," 1971. [Republished in *Chem. Eng. Commun.* **14,** 225 (1982)].
12. Hinch, E. J., and Acrivos, A., *J. Fluid Mech.* **98,** 305 (1980).
13. Rallison, J. M., *Ann. Rev. Fluid Mech.* **16,** 45 (1984).
14. Rallison, J. M., *J. Fluid Mech.* **98,** 625 (1980).
15. Guido, S., and Greco, F., *Rheol. Acta.* **40,** 176 (2001).

16. Taylor, G. I., *Proc. R. Soc. A London* **138,** 41 (1932).
17. Taylor, G. I., *Proc. R. Soc. A London* **146,** 501 (1934).
18. Cox, R. G., *J. Fluid Mech.* **37,** 601 (1969).
19. Torza, S., Cox, R. G., and Mason, S. G., *J. Colloid Interface Sci.* **38,** 395 (1972).
20. Guido, S., and Villone, M., *J. Rheol.* **42,** 395 (1998).
21. Guido, S., Greco, F., and Villone, M., *J. Colloid Interface Sci.* **219,** 298 (1999).
22. Rallison, J. M., *J. Fluid Mech.* **109,** 465 (1981).
23. Pozrikidis, C., *J. Fluid Mech.* **246,** 301 (1993).
24. Kennedy, M. R., Pozrikidis, C., and Skalak, R., *Comput. Fluids* **23,** 251 (1994).
25. Uijttewaal, W. S. J., and Nijhof, E., *J. Fluid Mech.* **302,** 45 (1995).
26. Loewenberg, M., and Hinch, E. J., *J. Fluid Mech.* **321,** 395 (1996).
27. Borhan, A., and Pallinti, J., *Phys. Fluids* **11,** 2846 (1999).
28. Toramaru, A., *Geophys. J. R. Ast. Soc.* **95,** 613 (1988).